Int. J. Electrochem. Sci., 14 **(2019)** 4066 – 4073, doi: 10.20964/2019.05.15

International Journal of
ELECTROCHEMICAL
SCIENCE
www.electrochemsci.org

Short Communication

Characterization and Intermediate Temperature Solid Oxide Fuel Cell Performances of $BaCe_{0.9}Tm_{0.1}O_{3-\alpha}$-KCl-NaCl Composite Electrolyte

Hui Miao[1,3], *Wei Chen*[2], *Wenli Hu*[2], *Hongtao Wang*[1,3,*]

[1] School of Chemical and Material Engineering, Fuyang Normal University, Fuyang 236037, China
[2] Fuyang Preschool Education College, Fuyang 236015, China
[3] Anhui Provincial Key Laboratory for Degradation and Monitoring of Pollution of the Environment, Fuyang 236037, China
[*]E-mail: hongtaoking3@163.com

Received: 31 January 2019 / *Accepted:* 5 March 2019 / *Published:* 10 April 2019

In this study, $BaCe_{0.9}Tm_{0.1}O_{3-\alpha}$ was prepared via a sol-gel combustion method using cerium nitrate, thulium oxide and barium nitrate as raw materials. Subsequently, it was reacted with the binary KCl-NaCl salts to obtain $BaCe_{0.9}Tm_{0.1}O_{3-\alpha}$-KCl-NaCl composite electrolyte. The structure, morphology, conductivity and fuel cell performance of the obtained samples were investigated. SEM images showed that KCl-NaCl inorganic molten salts covered and filled in the areas between the $BaCe_{0.9}Tm_{0.1}O_{3-\alpha}$ particles. The highest power density and conductivity of $BaCe_{0.9}Tm_{0.1}O_{3-\alpha}$-KCl-NaCl were 244.4 $mW \cdot cm^{-2}$ and 2.1×10^{-1} $S \cdot cm^{-1}$ $S \cdot cm^{-1}$ at 700 °C, respectively.

Keywords: Composite electrolyte; $BaCeO_3$; Molten salt; Fuel cell; Conductivity

1. INTRODUCTION

Electrolytes including oxygen-ion and protonic conductors as important components of solid oxide fuel cells (SOFCs) have attracted a great deal of research attention over the past decades [1-9]. SOFCs using oxygen-ion conductors as electrolytes usually require high operating temperature which limits their scope of application. Perovskite complex oxides have excellent protonic conductivities at high temperatures (700–1000 °C) and can be used in proton-conducting solid oxide fuel cells (PC-SOFCs) [10-15]. It is well known that $BaCeO_3$-based electrolytes have higher conductivities than $SrCeO_3$-based ceramics. Doping with low-valent metal ions, especially rare earth metal cations, can effectively improve the conduction properties of $BaCeO_3$-based electrolytes [16-19]. The ionic radius

ratio of Tm^{3+}/Ce^{4+} is 0.088 nm/0.087 nm = 1.01 in 6-fold coordination [20]. Therefore, $BaCe_{0.9}Tm_{0.1}O_{3-\alpha}$ was selected for this study.

It has been extensively proven that the electrochemical properties of electrolytes are influenced by the method of synthesis. The conventional method of synthesis for $BaCeO_3$-based electrolytes is solid-state reaction using cerium dioxide, barium carbonate and rare earth oxides as raw materials. Although this method of synthesis is simple, it requires high temperatures (1600–1700 °C). Usually, nanosized pure powders can be obtained by wet chemical preparations such as chemical precipitation, sol-gel combustion and microemulsion method etc. [21-23].

Medvedev et al. [24] reported that the addition of a phase to $BaCeO_3$-based electrolytes is the most effective strategy for improving the electrochemical properties of composites. Therefore, two-phase composite electrolytes with improved SOFC performances became a research hotspot [25-28]. Marques et al. combined $Ce_{0.5}Yb_{0.5}O_{1.75}$ with Li_2CO_3-Na_2CO_3 and the conductivities improved from 1.0×10^{-3} $S\cdot cm^{-1}$ ($Ce_{0.5}Yb_{0.5}O_{1.75}$ at 800 °C) to 0.1 $S\cdot cm^{-1}$ ($Ce_{0.5}Yb_{0.5}O_{1.75}$- Li_2CO_3-Na_2CO_3 at 500 °C) [26]. Park et al. investigated $BaZr_{0.85}Y_{0.15}O_{3-\delta}$-$Li_2CO_3$-$Na_2CO_3$ composite electrolyte which had excellent intermediate temperature electrochemical properties [27].

There are few studies about thulium-doped $BaCeO_3$. Therefore, in this study, $BaCe_{0.9}Tm_{0.1}O_{3-\alpha}$ was synthesized using a sol-gel combustion method. The corresponding composite electrolyte of $BaCe_{0.9}Tm_{0.1}O_{3-\alpha}$-KCl-NaCl was also prepared. Structural characterization and the intermediate temperature electrochemical properties of $BaCe_{0.9}Tm_{0.1}O_{3-\alpha}$ and $BaCe_{0.9}Tm_{0.1}O_{3-\alpha}$-KCl-NaCl were investigated.

2. EXPERIMENTAL

$BaCe_{0.9}Tm_{0.1}O_{3-\alpha}$ was synthesized via a sol-gel combustion method using cerium nitrate, thulium oxide, nitric acid, citric acid, ammonia and barium nitrate as raw materials. All the reagents used were analytical-grade (Shanghai Guoyao Group Chemical Reagents Co., Ltd.). Firstly, thulium oxide was dissolved in nitric acid and mixed with a metal nitrates solution in stoichiometric molar ratio. The barium nitrate: cerium nitrate: thulium oxide ratio was 1: 0.9: 0.1. Then, the citric acid solution was dropped as the chelating agent. The citric acid was three times as much as the total metal ion salts.The *p*H of the above solution was adjusted to 8-9 using ammonia. The water was evaporated until a solidified gel was obtained. Finally, after being combusted and sintered at 1250 °C and 1550 °C for 5 h, respectively, the $BaCe_{0.9}Tm_{0.1}O_{3-\alpha}$ was obtained [22, 29-31].

The mole ratio of KCl: NaCl was 1:1. The weight ratio of $BaCe_{0.9}Tm_{0.1}O_{3-\alpha}$: (KCl-NaCl) was 80:20. The resulting mixture was pelletized and calcined at 750 °C for 2 h to obtain $BaCe_{0.9}Tm_{0.1}O_{3-\alpha}$-KCl-NaCl composite electrolyte [32-33].

Thermogravimetric Analysis and Differential Scanning Calorimetry (TGA-DSC) was conducted before and after gel combustion of the $BaCe_{0.9}Tm_{0.1}O_{3-\alpha}$ precursor using a TA instrument. The initial mass of the $BaCe_{0.9}Tm_{0.1}O_{3-\alpha}$ precursor was 10 mg. The heat flow of DSC expressed the relationship of power difference vs. material quality between input sample and reference material. The atmosphere was of nitrogen and the heating rate was 15 $°C\cdot min^{-1}$from room temperature up to 1100

°C. The phase structures of $BaCe_{0.9}Tm_{0.1}O_{3-\alpha}$ and $BaCe_{0.9}Tm_{0.1}O_{3-\alpha}$-KCl-NaCl were analysed by a powder diffractometer. The morphological characteristics of $BaCe_{0.9}Tm_{0.1}O_{3-\alpha}$ and $BaCe_{0.9}Tm_{0.1}O_{3-\alpha}$-KCl-NaCl were examined using scanning electron microscopy (SEM) [23].

For impedance measurements, 20 % Pd-80 % Ag paste was painted onto both side surfaces (area: 0.5 cm^2) of $BaCe_{0.9}Tm_{0.1}O_{3-\alpha}$ and $BaCe_{0.9}Tm_{0.1}O_{3-\alpha}$-KCl-NaCl. The electrochemical impedance spectroscopy (R) was tested using an electrochemical analyser (CHI660E made in China) in air at 400–700 °C. Then, the conductivity could be calculated from: $\sigma = \frac{L}{R \cdot S}$, where σ is conductivity, R is resistance, L is thickness and S is area of electrolyte pellet. Finally, H_2/O_2 fuel cells of $BaCe_{0.9}Tm_{0.1}O_{3-\alpha}$ and $BaCe_{0.9}Tm_{0.1}O_{3-\alpha}$-KCl-NaCl (thickness: 1.1 mm) were investigated at 700 °C [29-33].

3. RESULTS AND DISCUSSION

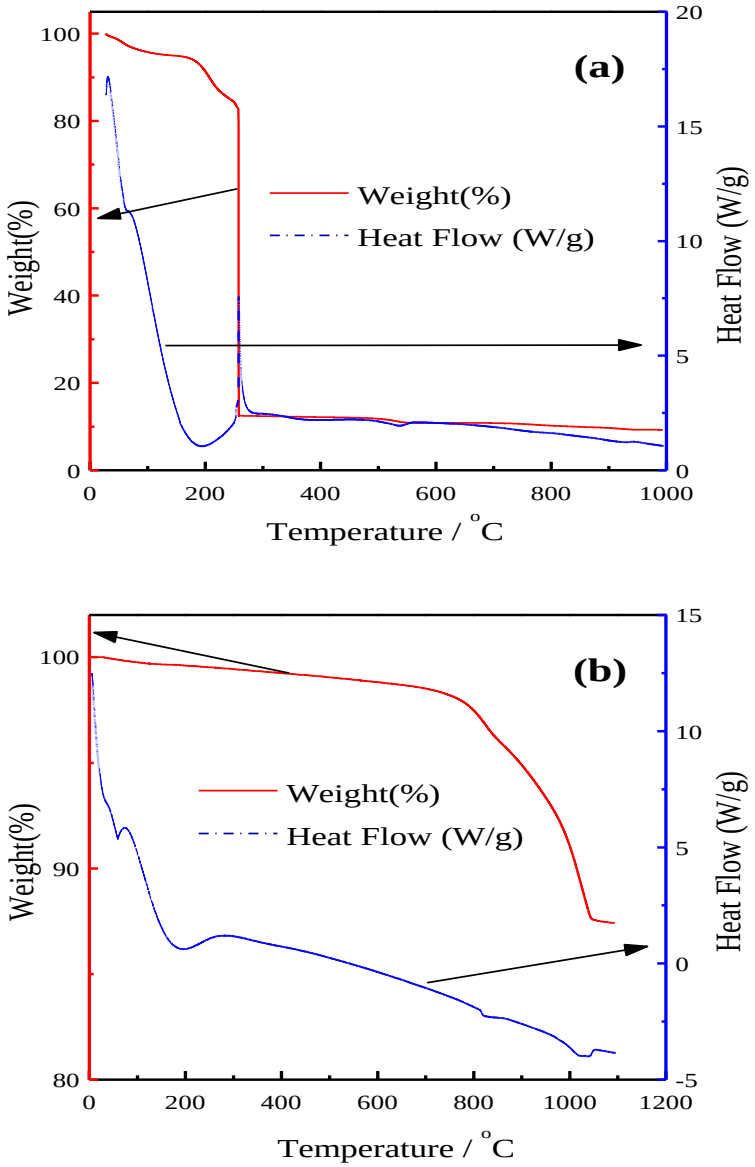

Figure 1. TGA-DSC curves before (a) and after (b) gel combustion of the $BaCe_{0.9}Tm_{0.1}O_{3-\alpha}$ precursor.

The TGA-DSC curves before (a) and after (b) gel combustion of the $BaCe_{0.9}Tm_{0.1}O_{3-\alpha}$ precursor are shown in Fig. 1. The atmosphere was of nitrogen and the heating rate was 15 °C·min^{-1}from room temperature up to 1100 °C. In Fig. 1(a), the 17 % weight loss up to 255 °C with a broad endothermic peak is ascribed to the absorption of ammonia, water and dehydration of organic compounds. The further 70 % weight loss accompanied by a sharp exothermic peak from 255 °C to 259 °C in DSC is attributed to the abrupt decomposition of citric acid [34]. From Fig. 1(b), the weight loss gently declined from room temperature to 300 °C accompanied by two endothermic peaks attributed to the incomplete decomposition of organic compounds. From 800 °C to 1050 °C, there is a 12 % weight loss accompanied by two weak endothermic peaks attributed to the incomplete decomposition of $BaCO_3$, polymorphic phase transformation and phase formation of $BaCe_{0.9}Tm_{0.1}O_{3-\alpha}$ [23].

Fig. 2 shows XRD patterns of $BaCe_{0.9}Tm_{0.1}O_{3-\alpha}$ (1250 °C and 1550 °C) and $BaCe_{0.9}Tm_{0.1}O_{3-\alpha}$-KCl-NaCl. According to the results of $BaCe_{0.9}Tm_{0.1}O_{3-\alpha}$ (1250 °C and 1550 °C), single orthorhombic $BaCeO_3$ (JCPDS 85-2155) phases are observed, which imply that the first synthetic temperature of 1250 °C was appropriate. Fig. 2 shows that $BaCe_{0.9}Tm_{0.1}O_{3-\alpha}$-KCl-NaCl has $BaCeO_3$, KCl (JCPDS 75-0296) and NaCl (JCPDS 88-2300) phases which indicates the chloride molten salts exist as crystalline phases in the composite electrolyte [29-32].

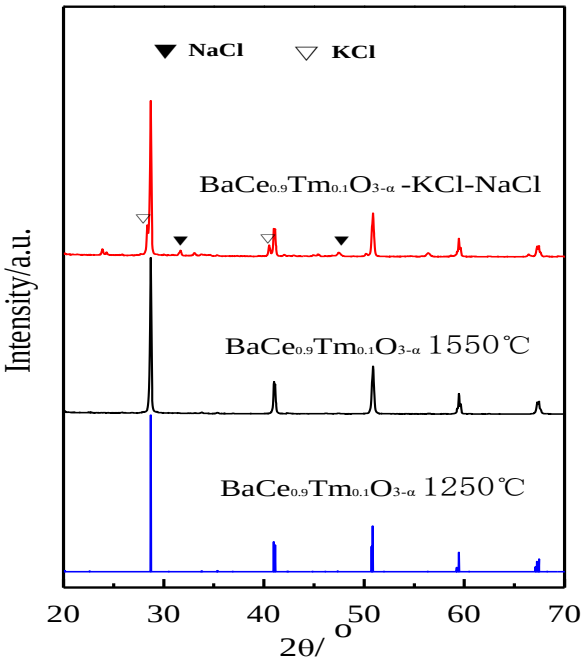

Figure 2. XRD patterns of $BaCe_{0.9}Tm_{0.1}O_{3-\alpha}$ (1250 °C and 1550 °C) and $BaCe_{0.9}Tm_{0.1}O_{3-\alpha}$-KCl-NaCl.

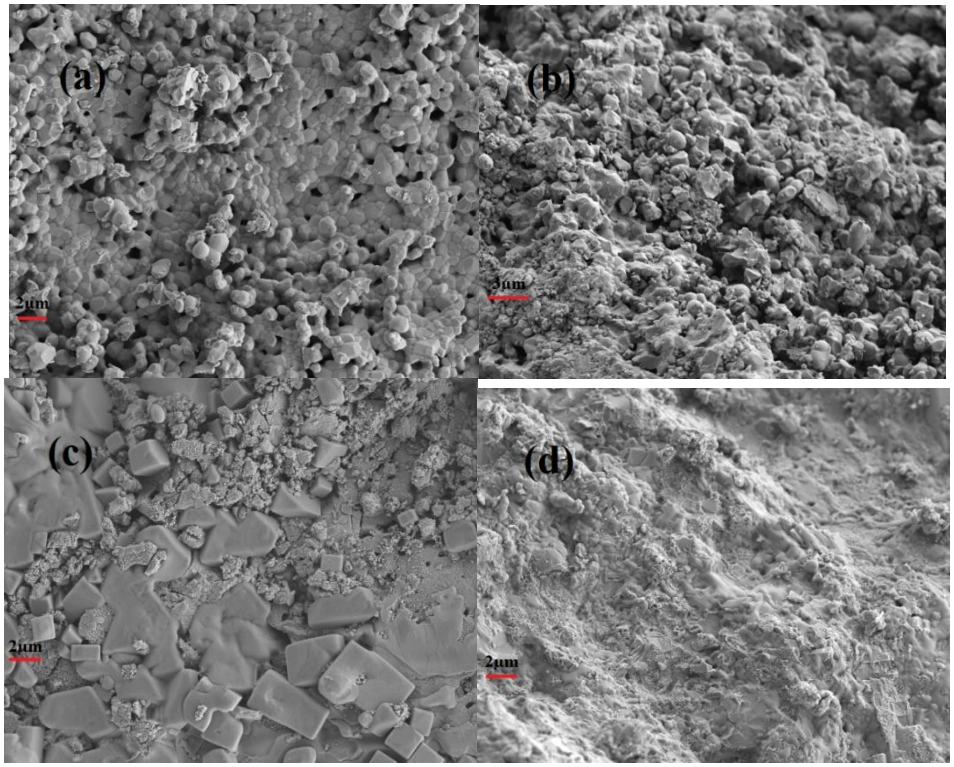

Figure 3. The SEM images of $BaCe_{0.9}Tm_{0.1}O_{3-\alpha}$ (1550 °C) (a,b) external and cross-sectional surfaces, and $BaCe_{0.9}Tm_{0.1}O_{3-\alpha}$-KCl-NaCl sintered at 750 °C for 2 h (c,d) external and cross-sectional surfaces.

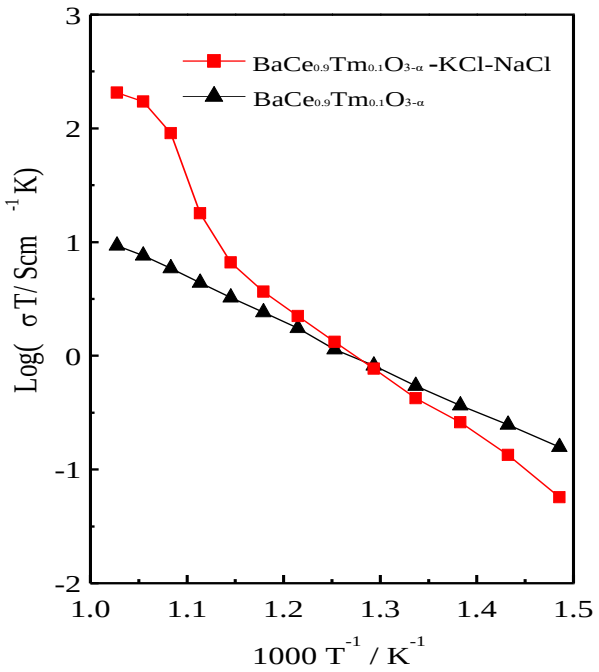

Figure 4. The conductivities of $BaCe_{0.9}Tm_{0.1}O_{3-\alpha}$ (1550 °C) and $BaCe_{0.9}Tm_{0.1}O_{3-\alpha}$-KCl-NaCl as a function of temperature in air from 400 °C to 700 °C.

The surface and cross-section SEM images of $BaCe_{0.9}Tm_{0.1}O_{3-\alpha}$ (1550 °C) and $BaCe_{0.9}Tm_{0.1}O_{3-\alpha}$-KCl-NaCl are displayed in Fig. 3. Fig. 3(a,b) shows the grain size range of sintered $BaCe_{0.9}Tm_{0.1}O_{3-\alpha}$ (1550 °C) pellet is 0.5-1.7μm. This shows that the sol-gel combustion method is advantageous to particle agglomeration. However, the grain boundary of $BaCe_{0.9}Tm_{0.1}O_{3-\alpha}$ (1550 °C) had not yet completely formed [23–25]. In the Fig. 3(c,d), it can be seen that the KCl-NaCl inorganic molten salts covered and filled in the areas between the $BaCe_{0.9}Tm_{0.1}O_{3-\alpha}$ particles promoting the sintering of the composite electrolyte [25–28].

The Arrhenius plots of $BaCe_{0.9}Tm_{0.1}O_{3-\alpha}$ (1550 °C) and $BaCe_{0.9}Tm_{0.1}O_{3-\alpha}$-KCl-NaCl as a function of temperature in air from 400 °C to 700 °C are recorded in Fig. 4. Within the test temperature range, the $BaCe_{0.9}Tm_{0.1}O_{3-\alpha}$ (1550 °C) agrees with the Arrhenius linear curve in air from 400 °C to 700 °C. The conductivity of $BaCe_{0.9}Tm_{0.1}O_{3-\alpha}$-KCl-NaCl ($2.1\times10^{-1}$ S·cm^{-1}) is much higher than that of $BaCe_{0.9}Tm_{0.1}O_{3-\alpha}$ (9.6×10^{-3} S·cm^{-1}) in air at 700 °C. The conductivities of $BaCe_{0.9}Tm_{0.1}O_{3-\alpha}$-KCl-NaCl show similar trends to previous reports [25–33], with sharp improvements near the melting point of inorganic salts. The results indicate that the molten KCl-NaCl salt provides more ion transport channels at high temperatures [24–28].

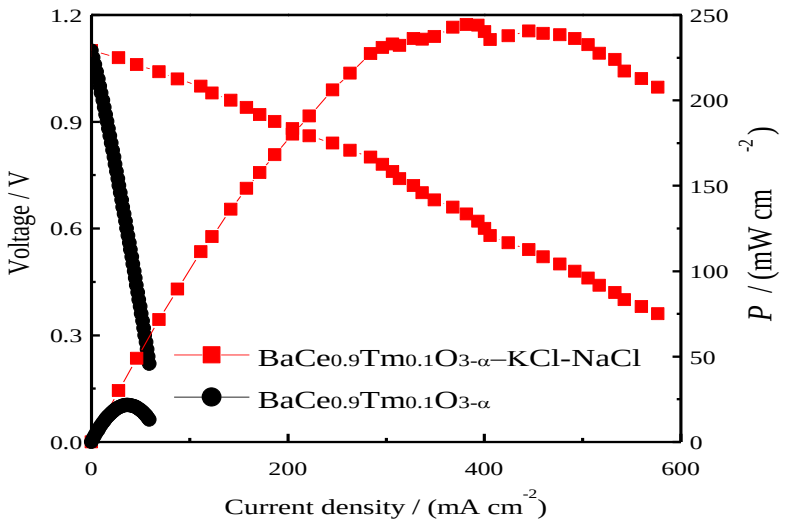

Figure 5. The *I-V-P* curves for H_2/O_2 fuel cells based on $BaCe_{0.9}Tm_{0.1}O_{3-\alpha}$ (1550 °C) and $BaCe_{0.9}Tm_{0.1}O_{3-\alpha}$-KCl-NaCl at 700 °C.

The *I-V-P* curves for H_2/O_2 fuel cells based on $BaCe_{0.9}Tm_{0.1}O_{3-\alpha}$ (1550 °C) and $BaCe_{0.9}Tm_{0.1}O_{3-\alpha}$-KCl-NaCl at 700 °C are shown in Fig. 5. As can be seen from Fig. 5, the open circuit voltages (OCVs) of $BaCe_{0.9}Tm_{0.1}O_{3-\alpha}$ (1550 °C) and $BaCe_{0.9}Tm_{0.1}O_{3-\alpha}$-KCl-NaCl are 1.1 and 1.09 V, respectively. This indicates that the molten phase fills in the remaining holes that may remain at 700 °C. The power density (*P*) of $BaCe_{0.9}Tm_{0.1}O_{3-\alpha}$-KCl-NaCl reaches 244.4 mW·cm^{-2}, which is higher than that of $BaCe_{0.9}Tm_{0.1}O_{3-\alpha}$ (21.6 mW·cm^{-2}) under the same conditions. For $BaCe_{0.9}Tm_{0.1}O_{3-\alpha}$-KCl-NaCl, molten salts may play important roles in improving fast conduction paths for carrier ions. The result is higher than the *P* values of $SrCe_{0.9}Eu_{0.1}O_{3-\alpha}$-NaCl-KCl (207 mW·cm^{-2}) [32] and

$SrCe_{0.9}Gd_{0.1}O_{3-\alpha}$-NaCl-KCl (215 mW·cm^{-2}) [33] at 700 °C. This may be due to the different electrolyte types.

4. CONCLUSIONS

In this study, $BaCe_{0.9}Tm_{0.1}O_{3-\alpha}$ was prepared via the sol-gel combustion method. XRD and TGA-DSC results indicated that the first synthetic temperature (1250 °C) for $BaCe_{0.9}Tm_{0.1}O_{3-\alpha}$ is appropriate. SEM images showed that KCl-NaCl inorganic molten salts covered and filled in the areas between the $BaCe_{0.9}Tm_{0.1}O_{3-\alpha}$ particles. The highest power density and conductivity of $BaCe_{0.9}Tm_{0.1}O_{3-\alpha}$-KCl-NaCl were 244.4 mW·cm^{-2} and 2.1×10^{-1} S·cm^{-1} S·cm^{-1} at 700 °C, respectively.

ACKNOWLEDGEMENTS
This work was supported by the National Natural Science Foundation (No. 51402052) of China, the Natural Science Foundation of Higher Education Institutions in Anhui Province (No. KJ2018A0332, KJ2018A0337, KJ2018A0980), Excellent Youth Foundation of Anhui Educational Committee (No. gxyq2018046), Horizontal cooperation project of Fuyang municipal government and Fuyang Normal College (No. XDHX2016013, XDHX2016019, XDHXTD201704).

References

1. G. L. Liu, W. Liu Q. Kou and S. J. Xiao, *Int. J. Electrochem. Sci*., 13 (2018) 2641.
2. Y. Yang, H. Hao, L. Zhang, C. Chen, Z. Luo, Z. Liu, Z. Yao, M. Cao and H. Liu, *Ceram. Int.*, 44 (2018) 11109.
3. Y. N. Chen, T. Tian, Z. H. Wan, F. Wu, J. T. Tan and M. Pan, *Int. J. Electrochem. Sci.*, 13 (2018) 3827.
4. T. Hibino, K. Kobayashi, P. Lv, M. Nagao, S. Teranishi, and T. Mori, *J. Electrochem. Soc.*, 164 (2017) F557.
5. S. Lee, and X. Guan, *MRS Communications.*, 7 (2017) 199.
6. J. Luo, A.H. Jensen, N.R. Brooks, J. Sniekers, M. Knipper, D. Aili, Q. Li, B. Vanroy, M. Wübbenhorst, F. Yan, L.V. Meervelt, Z. Shao, J. Fang, Z.-H. Luo, D.E.D. Vos, K. Binnemans, and J. Fransaer, *Energy Environ. Sci.*, 8 (2015) 1276.
7. A.A. Solovyev, S.V. Rabotkin, A.V. Shipilova and I.V. Ionov, *Int. J. Electrochem. Sci*., 14 (2019) 575.
8. C. Xia, Z. Qiao, C. Feng, J. Kim, B. Wang and B. Zhu, *Materials*, 11(2018) 40.
9. Y. Tian, Z. Lü, X. Guo and P. Wu, *Int. J. Electrochem. Sci*., 14 (2019) 1093.
10. Z. Zhang, L. Chen, Q. Li, T. Song, J. Su, B. Cai, H. He, *Solid State Ionic*s, 323 (2018) 25.
11. W. Wang, D. Medvedev and Z. Shao, *Adv. Funct. Mater.*, (2018) 1802592.
12. S.H. Morejudo, R. Zanón, S. Escolástico, I. Yuste-Tirados, H. Malerød-Fjeld, P.K. Vestre, W.G. Coors, A. Martínez, T. Norby, J.M. Serra and C. Kjølseth, *Science*, 353 (2016) 563.
13. E. Pikalova and D. Medvedev, *Int. J. Hydrogen Energ.*, 41 (2016) 4016.
14. S. Y. Bae, J.-Y. Park and H.-T. Lim, *Electrochim. Acta*, 236 (2017) 399.
15. H. Sun, S. Zhang, C. Li, B. Rainwater, Y. Liu, L. Zhang, Y. Zhang, C. Li and M. Liu, *Ceram. Int.*, 42 (2016) 19231.
16. N. Danilov, E. Pikalova, J. Lyagaeva, B. Antonov, D. Medvedev, A. Demin and P. Tsiakaras, *J. Power Sources*, 366(2017) 161.
17. J. Xiao, L. Chen, H. Yuan, L. Ji, C. Xiong, J. Ma and X. Zhu, *Mater. Lett.*, 189 (2017) 192.

18. J. Lyagaeva, G. Vdovin, L. Hakimova, D. Medvedev, A. Demin and P. Tsiakaras, *Electrochim. Acta*, 251 (2017) 554.
19. G. S. Reddy and R. Bauri, *J. Alloy Compd.*, 688 (2016) 1039.
20. R.D. Shannon, *Acta Cryst.*, A32 (1976) 751.
21. J.M. Sailaja, K.V. Babu, N. Murali, and V. Veeraiah, *J. Adv. Res.*, 8 (2017) 169.
22. J. Song, B. Meng and X. Tan, *Ceram. Int.*, 42 (2016) 13278.
23. J.M. Sailaja, N. Murali, S.J. Margarette, T.W. Mammo and V. Veeraiah, *Results Phys.*, 8 (2018) 128.
24. D.A. Medvedev, J.G. Lyagaeva, E.V. Gorbova, A.K. Demin and P. Tsiakaras, *Prog. Mater. Sci.*, 75 (2016) 38.
25. A.I.B. Rondao, S.G. Patricio, F.M.L. Figueiredo and F.M.B. Marques, *Int. J. Hydrogen Energ.*, 39 (2014) 5460.
26. N.C.T. Martins, S. Rajesh and F.M.B. Marques, *Mater. Res. Bull.*, 70 (2015) 449.
27. K.-Y. Park, T.-H. Lee, J.-T. Kim, N. Lee, Y. Seo, S.-J. Song and J.-Y. Park, *J. Alloy Compd.*, 585 (2014) 103.
28. Y. Hei, J. Huang, C. Wang and Z. Mao, *Int. J. Hydrogen Energ.*, 39 (2014) 14328.
29. W. Zhang, M. Yuan, H. Wang and J. Liu, *J. Alloy Compd.*, 677(2016) 38.
30. R. Shi, J. Liu, H. Wang, F. Wu and H. Miao, *Ceram. Int.*, 43 (2017) 16931.
31. Q. Guan, H. Wang, H. Miao, L. Sheng and H. Li, *Ceram. Int.*, 43 (2017) 9317.
32. R. Shi, J. Liu, H. Wang, F. Wu, H. Miao and Y. Cui, *Int. J. Electrochem. Sci.*, 12 (2017) 11594.
33. L. Sun, H. Wang, L. Sheng and H. Li, *Int. J. Electrochem. Sci.*, 12 (2017) 9689.
34. A. Matsuda, S. Oh, V.H. Nguyen, Y. Daiko, G. Kawamura and H. Muto, *Electrochim. Acta*, 56 (2011) 9364.